Statistical *n*-Butyl Acrylate–(Sulfopropyl)ammonium Betaine Copolymers. 4. Dynamic Mechanical Properties

Marc Ehrmann,† René Muller,† Jean-Claude Galin,† and C. Geraldine Bazuin*,‡

Institut Charles Sadron (CRM-EAHP), CNRS-ULP, 6, rue Boussingault, 67083 Strasbourg Cedex, France, and Centre de recherche en sciences et ingénierie des macromolécules (CERSIM), Département de chimie, Université Laval, Québec, Canada G1K 7P4

Received December 31, 1992; Revised Manuscript Received June 3, 1993

ABSTRACT: The dynamic mechanical behavior of butyl acrylate-based zwitterionomers from the glassy to the terminal zones is described. Two T_g's had been detected previously by differential scanning calorimetry (DSC) for zwitterion contents, F_B, above 4.5 mol %. The biphasic morphology of these materials and the increasing importance of the "hard" phase relative to the "soft" phase are confirmed. The glass transition of the soft phase (T_g^S) increases by only 1.5 °C/mol % zwitterion content. A well-defined rubbery zone is evident, whose pseudoequilibrium modulus increases as $G_N^\circ \propto F_B^{2.2}$. The terminal zone is increasingly retarded to higher temperatures or lower frequencies (thus extending the rubbery plateau range) with zwitterion content. An unusual feature of the moduli–frequency curves is the appearance of a zone of constant slope intermediate to the rubber and terminal zones. The addition of a stoichiometric amount of $LiClO_4$ further extends the length of the rubbery plateau zone but has little effect either on the T_g^S or on the rubbery modulus. This indicates that the salt enhances the strength of the zwitterionic interactions but does not enhance phase separation. All samples appear to be thermorheologically simple; however, the shift factors fit a simple WLF equation only at low zwitterion contents.

Introduction

Zwitterionomers, with both cationic and anionic units covalently incorporated into the polymer, have received far less attention from the scientific community to date than ionomers, which possess only cationic or only anionic covalently-attached units. Several zwitterionomers which have been reported in the literature were shown to have a biphasic morphology[1-4] similar to that of ionomers.[5-7] The presence of the oppositely-charged ionic groups (often on the same pendant group), the option of adding inorganic salts, and the fact that the pendant groups are longer than those in most ionomers render a detailed investigation of these materials of interest.

This paper presents the fourth in a series of studies of statistical zwitterionic copolymers of *n*-butyl acrylate (A) and dimethyl(3-methacrylamidopropyl)(3-sulfopropyl)-ammonium betaine (B): Structural studies[8,9] using dif-

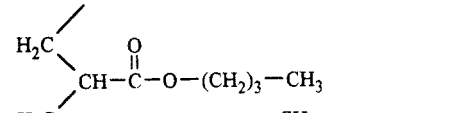

(A)

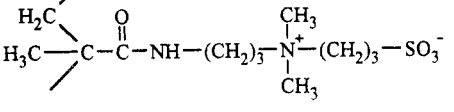

(B)

ferential scanning calorimetry (DSC), small-angle X-ray scattering (SAXS), and solid-state NMR have shown that these materials are biphasic. Of particular interest is the fact, rarely seen for ionomers, that two T_g's are clearly detected by DSC for B contents between 4.5 and 40 mol %. They are referred to as T_g^S for the "soft" phase and T_g^H for the "hard" phase. The soft phase was shown to be relatively pure, with less than 0.07 molar fraction B content. The hard phase, on the other hand, was shown to be chemically heterogeneous, with a relatively high A content (between 0.4 and 0.7 molar fraction). The phase segregation is attributed to the strong dipole–dipole interactions among the zwitterions ($\mu \approx 25$ D) within a low polarity, highly mobile matrix [the glass transition of poly(*n*-butyl acrylate) is −46.5 °C], thereby creating regions of reduced segmental mobility (the hard phase), in accordance with the most recent model of ionomer morphology.[7] SAXS profiles show a typical "ionomer peak", corresponding to Bragg spacings of 3–8 nm, which does not disappear even 100 °C above the T_g^H.

In order to more closely compare these zwitterionomers with classical ionomers, this paper describes their dynamic mechanical properties. These properties have traditionally provided the main source of evidence for the biphasic character of ionomers and indicate both the extent of phase segregation and the strength of ionic interactions.[5-7] The investigation will be restricted to B contents typical of classical ionomers (<15 mol %), where the homopolymer, poly(*n*-butyl acrylate), serves as a reference. The copolymer compositions to be studied are 2 mol % (indicated to be homogeneous and monophasic according to both DSC and SAXS measurements), 4 mol % (monophasic according to DSC but microheterogeneous according to SAXS), and 7.1 and 12.8 mol % (biphasic copolymers according to both DSC and SAXS), as well as a mixture of the 7.1% copolymer with a stoichiometric amount of $LiClO_4$ ([$LiClO_4$]/[B] = 1). The results will also be compared to a previously studied poly(ethyl acrylate)-based zwitterionomer system.[4]

Experimental Section

Synthesis and Sample Preparation. The free-radical polymerization of the monomers A and B, restricted to conversions of less than 15%, and the molecular characterization of the copolymers have been described in the first paper of this series.[10] The samples will be referred to as AB-*x*, where *x* represents the mol % B content, e.g., AB-7.1 for the copolymer containing 7.1 mol % B. The stoichiometric blend of AB-7.1 with $LiClO_4$, to be referred to as AB′-7.1, was obtained by evaporation of their dilute solution in trifluoroethanol. The samples were dried at 80 °C under a vacuum of *ca.* 10^{-2} Torr for 24 h. The molecular

* To whom correspondence should be addressed.
† Institut Charles Sadron.
‡ Université Laval.

0024-9297/93/2226-4910$04.00/0

Table I. Molecular and Morphological Characteristics of the Samples Studied[a]

	W_B	$\overline{DP}_w$	$\overline{M}_w/\overline{M}_n$	T_g (°C)	ΔT (°C)	W^H	W_B^S	W_B^H
A	0	2200	2.4	−46	9	0	0	0
AB-2.0	0.045	2020		−43	11	0.07[b]	0.02[b]	0.38[b]
AB-4.0	0.087	1940	2.2	−40	14	0.13[b]	0.03[b]	0.42[b]
AB-7.1	0.148	1900	2.2	−38	19	0.202	0.060	0.498
				+44	22			
AB-12.8	0.250	1850	1.8	−36	18	0.387	0.074	0.529
				+52	19			
AB′-7.1	0.148	1900	2.2	−37	20	0.202	0.060	0.498
				+59	35			

[a] W_B: weight fraction of B in the sample. W^H: weight fraction of hard phase in the sample. W_B^S, W_B^H: weight fractions of B in the soft and hard phases, respectively. ΔT: width of the glass transition. [b] Values extrapolated for hypothetical soft and hard phases from equations[8] correlating T_g^S and T_g^H as a function of W_B: T_g^S(°C) = −46.4 + 52.3W_B and T_g^H(°C) = 5.1 + 238W_B.

and structural characteristics of the copolymers studied, as determined in refs 8 and 10, are given in Table I. The degrees of polymerization are similar in all cases (2000 ± 200), as are their molecular weight distributions (M_w/M_n = 2.0 ± 0.2).

The samples were molded at 100 °C (120 °C for AB′-7.1) for 1 h under several atmospheres of pressure, after having been degassed for 1 h at 30 °C. Those of 4 mol % B content or less were unmolded by dipping in liquid nitrogen; the others were easily unmolded at ambient temperature. The molded samples had a slight yellow tint and became increasingly translucent as B content increased.

Dynamic Mechanical Analysis. The Polymer Laboratories dynamic mechanical thermal analyzer (DMTA), MK2, and the Rheometrics mechanical spectrometer (RMS), RMS-605, were used for dynamic mechanical and rheological measurements.

The DMTA was operated in sinusoidal tensile bending mode at a nominal peak-to-peak deflection of 64 μm using a dual cantilever. Measurements were taken at five frequencies (0.3, 1, 3, 10, 30 Hz) as a function of temperature at a heating rate of 0.7 °C min^{-1}. The rectangular bar-shaped samples were typically 10 mm wide by 2 mm thick with a free length of 5 mm. The sample chamber was constantly flushed with a light flow of dry nitrogen.

The RMS was operated in the sinusoidal shear mode as a function of frequency (0.1–100 rad s^{-1}; 5–10 frequencies per decade) at various temperatures (between −100 and +195 °C in 5–20 °C steps). Measurements around the glass transition temperature (T_g or T_g^S) were made on rectangular specimens (40 × 12 × 3 mm) subjected to torsion. Parallel plates were used above the T_g. The rubbery plateau region (−30 to +60 °C) was measured using disk-shaped specimens of 10 mm diameter and 0.6 mm thickness, and the flow region (20–195 °C) using disk-shaped specimens of 25 mm diameter and 1 mm thickness. In order to assure good adhesion between the sample and the surfaces of the parallel plates, the AB samples were put into place at 100 °C and the AB′ sample at 150 °C.

It was not possible to make RMS measurements on a rectangular bar of pure poly(*n*-butyl acrylate) around its T_g, because of its extreme softness at room temperature and brittleness when cooled with liquid nitrogen. Some RMS measurements near the T_g were made using grooved parallel plates. However, this probably results in high-frequency values that are inaccurate due to imperfect adhesion; furthermore, transducer limits restricted the measurements to modulus values of less than 10^8 Pa.

In all of the RMS measurements, the sample chamber was flushed with a constant flow of dry nitrogen. The amplitude of deformation for the RMS measurements was ensured to be sufficiently weak that the response of the material was in the linear viscoelastic regime. Moreover, the measurements were generally reproducible and independent of the thermal history of the sample; it was verified, for example, that the frequency measurements on a sample at 25 °C gave essentially the same results before and after the series of measurements up to 180 °C were taken.

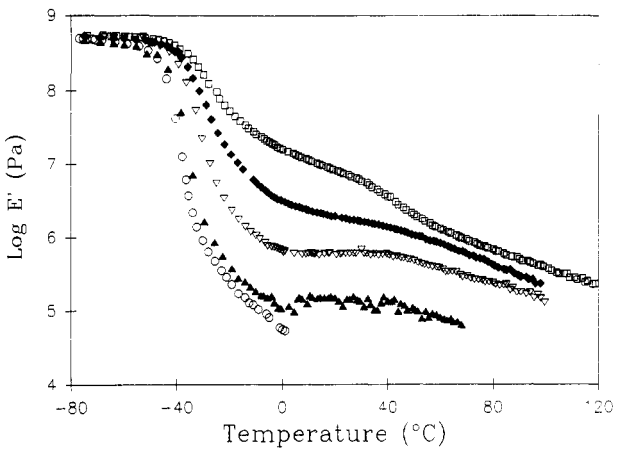

Figure 1. Young's storage modulus at 1 Hz as a function of temperature for: ○, A; ▲, AB-2.0; ▽, AB-4.0; ◆, AB-7.1; □, AB-12.8.

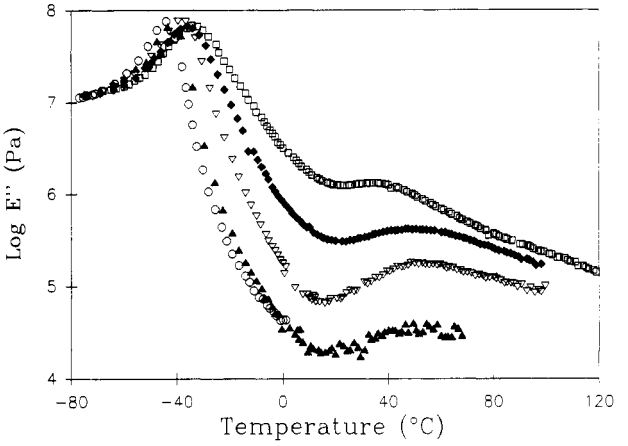

Figure 2. Young's loss modulus at 1 Hz as a function of temperature for the samples identified in Figure 1.

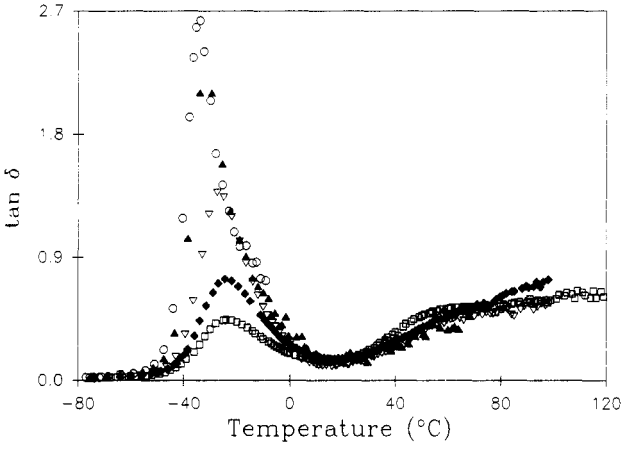

Figure 3. Loss tangent at 1 Hz as a function of temperature, measured by DMTA, for the samples identified in Figure 1.

Results and Discussion

Thermal Analysis. The Young's storage moduli (E'), loss moduli (E''), and loss tangents (tan δ) as a function of temperature at a frequency of 1 Hz, obtained from the DMTA, are shown in Figures 1–3 for poly(*n*-butyl acrylate) (PBA) and the four copolymers studied. For comparison, the loss tangent results obtained by RMS on rectangular bars for the four copolymers are shown in Figure 4.

As was observed in studies of poly(ethyl acrylate) (PEA) zwitterionomers,[4] and as is observed for biphasic ionomers in general,[5] the storage moduli curves in Figure 1 show that the glass transition zone of the PBA zwitterionomers

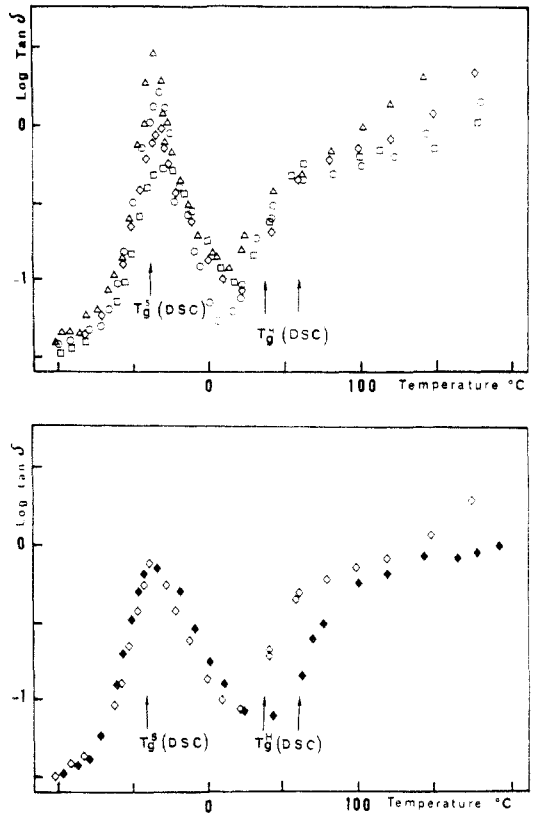

Figure 4. Loss tangent at 1 Hz as a function of temperature, measured by RMS: △, AB-2.0; ○, AB-4.0; ◇, AB-7.1; □, AB-12.8; ◆, AB′-7.1. The arrows indicate the glass transitions of the soft (T_g^S) and hard (T_g^H) phases of AB-7.1, AB-12.8, and AB′-7.1, as obtained from DSC.[8]

increases somewhat in temperature, and its slope decreases significantly, with increasing zwitterion content. A higher temperature transition is clearly evident at *ca.* 50 °C in AB-12.8. Furthermore, a broad rubbery plateau zone is apparent for all zwitterionomers, even for AB-2.0; its modulus increases dramatically as the zwitterion content increases. For AB-2.0 and AB-4.0, this rubbery plateau is approximately constant in modulus over a range of *ca.* 50 °C. The readily distinct rubbery zone in the PBA zwitterionomers contrasts with that observed in the PEA zwitterionomers and in many ionomers, where demarcation between the transition and the rubbery zones is less clearly marked. On the other hand, in the case of the PEA zwitterionomers, the addition of a stoichiometric amount of a low molecular weight salt, $LiClO_4$, did produce an extended rubbery plateau,[4] resulting in curves remarkably similar to those of the salt-free PBA zwitterionomers of this study.

In Figure 3, it is observed that the intensity of the loss tangent maximum reflecting the PBA glass transition decreases significantly with increase in zwitterion content. This is again similar to what was reported for the PEA zwitterionomers[4] and to what is generally observed in biphasic ionomers.[5] It reflects the progressive decrease in volume fraction of the matrix or soft phase as ion or zwitterion content increases. The half-widths of these peaks (but not the base widths) increase with zwitterion content, paralleling the DSC results concerning the T_g width (Table I). The temperature corresponding to the loss tangent maximum increases only mildly with zwitterion content (*ca.* 1 °C/mol %), also paralleling the T_g (or T_g^S) trends of this system as observed by DSC. This increase in T_g is less than is usually observed in ionomers;[5] even the T_g's of styrene-based ionomers whose ionic groups are at the end of relatively long pendant chains increase by 3–5 °C/mol % ion content.[11] The small increase in T_g for the zwitterionomers is consistent with the relative purity of the A phase as determined from DSC data.[8] The comparison with the ionomers indicates that the matrix phase of the PBA zwitterionomers is much more devoid of zwitterionic groups than are most ionomers of ionic groups.[12] Significantly, one exception reported in the literature is a vinylpyridinium ionomer, a biphasic ionomer also based on butyl acrylate, whose T_g similarly increases at a rate of 1 °C/mol % ion content.[13]

In biphasic ionomers, a higher temperature loss tangent peak is frequently observed in dynamic mechanical studies.[5,6,11,14] It is identified as the glass transition of a second phase, often called a cluster phase or clusters or microphase-separated regions, where the chain mobility is reduced due to the strong electrostatic interactions.[7] Since the present system has already been shown by DSC to possess two T_g's, of which the higher temperature one was considered to be related to a clustered or hard phase,[8] it is expected that this will also be visible in DMTA measurements. However, Figure 3 shows that a higher temperature loss tangent peak is not clearly evident. On the other hand, the loss tangent curves increase sharply (and similarly) in intensity between *ca.* 30 and 60 °C, followed by a much more gradual increase, for all four copolymers. For AB-12.8, the loss tangent values above *ca.* 50 °C are higher than that of the T_g maximum. Increasing dominance of the higher temperature transition relative to the glass transition as ion content increases is commonly observed in biphasic ionomers.[14] Phenomena similar to those above were noted for the PEA zwitterionomers.[4]

As shown in Figure 4, loss tangent curves obtained from RMS torsional measurements are essentially identical to those obtained from DMTA. The glass transition temperatures, as determined by DSC,[8] are also indicated in this figure. It can be observed that in the cases for which a T_g^H could be detected by DSC, it lies near the beginning of the second rise in the loss tangent curves. The T_g^S measured by DSC is located close to the low-temperature loss peak maximum in all cases. The widths of the latter peak at half-height (25, 32, 36, and 47 °C for AB-2.0, AB-4.0, AB-7.1 and AB-12.8, respectively) and their areas (76, 51, 33, and 23, in arbitrary units, for AB-2.0, AB-4.0, AB-7.1, and AB-12.8, respectively) are increasing and decreasing functions, respectively, of zwitterion content.

These *is* evidence of a maximum above the T_g in the loss modulus curves (Figure 2), including that for AB-2.0. This peak is centered at *ca.* 50 °C for the three lower zwitterion contents and at *ca.* 35 °C for AB-12.8. It can be related to the T_g^H observed in DSC and identified with regions of reduced mobility in these materials.

The fact that no second T_g was observed through DSC in AB-2.0 and AB-4.0, for which an E'' peak is visible by DMTA, may be due to insufficient total volume and/or average domain size of the second phase for detection by DSC (notice the W^H values in Table I); the DMTA method is apparently more sensitive. This is all the more plausible given that it is rare that biphasic ionomers in general, for which two dispersion regions are detected dynamic mechanically, show more than one T_g through DSC. A characteristic small-angle X-ray scattering peak for the PBA system is evident for zwitterion contents of *ca.* 4 mol % and above,[8] indicating a sensitivity to zwitterion aggregates intermediate to the sensitivity of DMTA and DSC to the hard phase.

Apparent Arrhenius activation energies for the two DMTA transitions were determined to be *ca.* 180 kJ mol^{-1} (from the loss tangent maxima) and *ca.* 100 kJ mol^{-1} (from

the loss modulus maxima, since corresponding maxima cannot be clearly identified in the loss tangent data) for the T_g^S and T_g^H, respectively. No significant variation with zwitterion content was observed. Again, the higher energies noted for the lower transition compared to the higher transition appear to be typical of biphasic ionomers in general and have been taken as supportive evidence for the existence of two phases, each with its own T_g, in these materials.[14]

A DMTA scan of AB'-7.1, the 7.1% zwitterionomer to which a stoichiometric quantity of $LiClO_4$ was added, does not show large changes from the scan of the salt-free zwitterionomer. The main difference is that the second rise in the loss tangent is delayed by *ca.* 20 °C (Figure 4); in the PEA zwitterionomers, there was more than a 40 °C delay.[4] In both PBA and PEA zwitterionomers, the glass transition is affected very little by the addition of salt.

Thus, dynamic mechanical thermal analysis confirms that the PBA zwitterionomers are biphasic and that their behavior is qualitatively similar to that of biphasic ionomers. It also indicates, from the length of the rubbery plateau, that the electrostatic interactions are very strong and that ion-hopping is not significant until elevated temperatures. Some quantitative aspects will be treated below.

Frequency Analysis. The storage and loss moduli of the samples were measured from the glass transition to flow zones as a function of frequency ($0.1–10^2$ rad s^{-1}) at various temperatures, using the RMS. Master curves were constructed, choosing T_g^S + 60 °C (as determined from DSC) as the reference temperature or T_g + 60 °C in the case of the polymers with a single glass transition. These master curves are shown in Figure 5. In almost all cases, complete superposition of the isotherms was possible by appropriate horizontal displacements accompanied by small vertical displacements. The vertical displacements (*ca.* 0.01 logarithmic units per 10 °C) correspond to the term $\log \rho_0 T_0/\rho T$ where ρ_0 and ρ are the densities of the material at temperatures T_0 and T, respectively, and T_0 is the reference temperature. The only exceptions to superposition occur near the glassy zone for A, AB-2.0, and AB-12.8; but this can most likely be attributed to experimental difficulties.

The validity of the time-temperature superposition principle suggests that the materials are thermorheologically simple. This was also observed for the poly(ethyl acrylate)-based zwitterionomers both with and without added salt.[4] Ionomers have frequently been found to be thermorheologically complex,[5] in particular in an ion content range which is now thought to be that where the two phases, each with relaxation processes with different time dependences, are cocontinuous.[14] This may indicate that the cluster phase in the zwitterionomers in the composition range studied is not yet sufficiently dominant that additional relaxation processes are rheologically effective. On the other hand, it is possible that thermorheological complexity in the zwitterionomers has simply gone undetected due to the limited frequency range employed; many of the ionomer studies in which time–temperature superposition was observed to fail were conducted as stress relaxation experiments over wider frequency/time ranges than those investigated here.

It is to be noted that the entry into the terminal zone, as indicated by the crossover point of the storage and loss moduli curves, is very far from the glass transition zone and is increasingly displaced to lower frequencies (or higher temperatures) with increasing zwitterion content. The crossover point for AB'-7.1 is also at lower frequencies

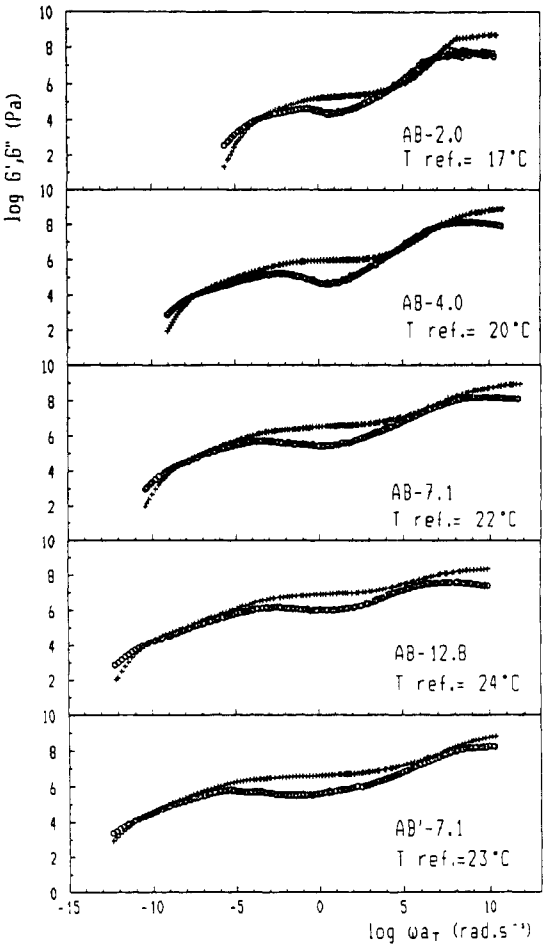

Figure 5. Master curves of the shear moduli (+, storage; O, loss) reduced to T_g^S+60 °C.

than that for AB-7.1. This is consistent with the observations made above concerning the temperature range of the rubbery zone in thermal analysis.

The storage and loss moduli curves are collected separately as a function of zwitterion content in Figure 6. In comparison with the PBA homopolymer, the rubbery modulus of the zwitterionomers (Figure 6a) increases significantly with zwitterion content, as much as 2 orders of magnitude at 12.8%. In parallel to this, the width of the rubbery zone increases toward lower frequencies: if the inflection point between the glass transition and rubbery zones and the subsequent inflection point are taken to delimit the width of the rubbery zone, it is observed that, whereas the first inflection point remains approximately constant in frequency (at *ca.* 10^4 rad s^{-1}), the second one decreases from 1 rad s^{-1} for AB-2.0 to 10^{-3} rad s^{-1} for AB-12.8 at a reference temperature of T_g + 60 °C.

The loss modulus in the rubbery plateau zone also increases with zwitterion content, especially for AB-7.1 and AB-12.8 (Figure 6b). This is particularly evident from observation of the loss modulus minimum present for all the zwitterionomers and which remains relatively constant in frequency at *ca.* 5 rad s^{-1}. This minimum is the deepest for the copolymers of lower zwitterion content, despite the fact that the width of the rubbery zone is smaller for these copolymers.

Following the rubbery plateau zone (in the direction of lower frequencies), it can be observed (Figure 6b) that G'' passes through a maximum, generally a little beyond the second inflection point in the G' curves mentioned above. It is noteworthy that, whereas the G'' maximum tends to

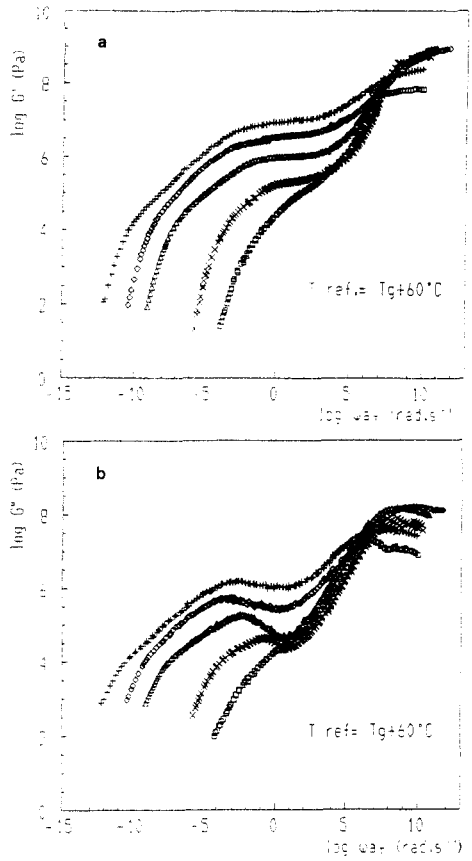

Figure 6. Master curves of the shear and loss storage moduli reduced to T_g^S+60 °C: □, A; ×, AB-2.0, △, AB-4.0; ◇, AB-7.1; +, AB-12.8.

decrease in frequency with increase in zwitterion content, that for AB-12.8 is located at a higher frequency than that for AB-7.1. This corresponds to the general (linear) increase in temperature with increasing zwitterion content observed for the T_g^H determined by DSC, with the observation that the T_g^H for AB-12.8 lies significantly below the line representing the average increase.[8] It was noted in Figure 2 that the E'' maximum for AB-12.8 was also lower in temperature than that for AB-7.1. This consistency between all three methods, for which the samples were prepared separately, suggests that the lower temperature (or higher frequency) of the transition is intrinsic to the sample and not a result of thermal treatment. (Perhaps a polar impurity, such as residual zwitterionic monomer, is present that causes some plasticization of the hard phase.[15])

The slopes of both the G' and G'' curves beyond the inflection point and maximum, respectively, are relatively constant for several decades of frequency before entering the terminal zone. The higher the zwitterion content, the longer this slope. This region corresponds to that of the relatively flat plateau at the higher temperatures in the thermal loss tangent curves (Figures 3 and 4). The slopes of the moduli can be related to the frequency by a power law of the type $G',G'' \propto \omega^n$. The value of n for the G' curves in this zone is about 0.35; for the G'' curves, this value is somewhat lower (see Figure 5), ranging from 0.25 for AB-2.0 to 0.31 for AB-12.8.

Dynamic rheological data of classical ionomers published in the literature were examined for similar behavior. Only one example was found, uncommented on, where such a slope between the rubbery and terminal zones is evident, namely, for a 5 mol % polystyrene ionomer plasticized by 40 wt % styrene oligomer;[16] in this case n = 0.3. Stadler

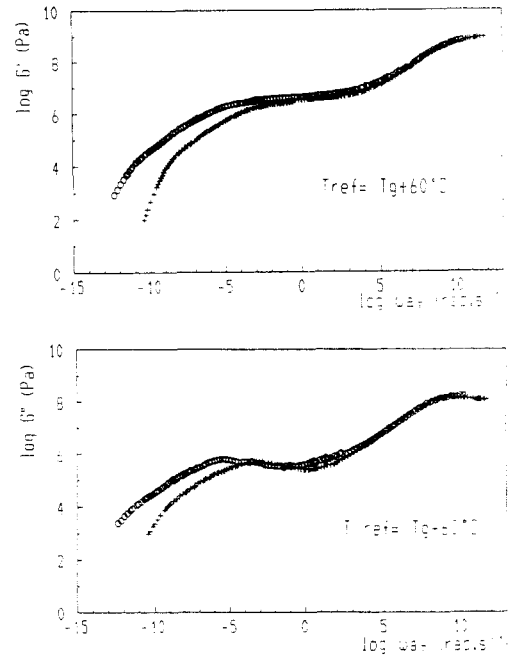

Figure 7. Master curves of the storage and loss shear moduli reduced to T_g^S+60 °C: +, AB-7.1; ○, AB′-7.1.

and de Lucca Freitas[17] observed such a slope for polybutadienes functionalized to 1 and 2 mol % by urazole groups; strong hydrogen-bonding associations result in a material with thermoreversible cross-linking behavior. In their case, the values of n are 0.55–0.88, decreasing with increase in functionalization; the terminal zone, as indicated by slopes of 1 and 2 for G' and G'', respectively, was not attained for the 2 mol % material. For the salt-free zwitterionomers of our study, the terminal zone generally is attained; it occurs in frequency ranges (relative to T_g + 60 °C) between 10^{-6} and 10^{-12} rad s^{-1}.

When salt is added to AB-7.1 (Figure 7), there is little change in the glass transition zone, consistent with the thermal analysis results. The rubbery zone is clearly extended to lower frequencies (the second inflection point in G' and the minimum in G'' are displaced by *ca.* 2 decades); however, the height of the rubbery plateau is similar with and without salt. Furthermore, the constant slope in the zone between the rubbery and terminal zones is still present for AB′-7.1. The value of the slope is similar to that for AB-7.1, although it is somewhat extended in length with the addition of salt. In fact, the terminal zone for AB′-7.1 is barely attained compared to the salt-free zwitterionomer; at the highest temperature isotherm measured for AB′-7.1, 195 °C, the material begins to degrade, and the slopes measured at that point are only 1.0 for G' and 0.6 for G'' in frequency ranges between 10^{-11} and 10^{-13} rad s^{-1} (relative to T_g + 60 °C). The salt appears to have little effect on the extent of phase segregation, as indicated by the height of the rubbery plateau; rather, it increases the strength of the aggregates, or increases their lifetimes, so that flow is significantly retarded.

Some aspects of the rheological behavior of the PBA zwitterionomers described above resemble that for the PEA zwitterionomers;[4] other aspects do not. In both cases, the modulus of the rubbery zone increases with increasing zwitterion content and the terminal zone tends to be retarded to lower frequencies. However, no minimum in the G'' curve was observed for the PEA zwitterionomers, nor did they show the constant slope intermediate to the rubbery and flow zones. This is probably due at least in part to the closer proximity of the two T_g's in the PEA

Table II. Results of Calculations Related to the Rubbery Plateau (see Text for Details)

sample	$G_N^\circ \times 10^{-5}$ (Pa)	$G \times 10^{-5}$ (Pa)	ν_e	$G_m \times 10^{-5}$ (Pa)	M_e	M_e'/M_e	$(\bar{r_0^2})^{0.5}$ (Å)	d_{SAXS} (Å)
AB-2.0	2.2	1.8	0.06	2.0	10 600	0.6	70	
AB-4.0	9.7	2.0	0.25	8.2	2 600	1.3	35	71
AB-7.1	38.7	2.6	0.75	24.8	900	2.2	20	65
AB-12.8	119.6	4.0	1.51	49.7	400	2.9	15	54

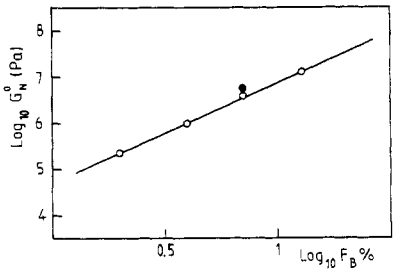

Figure 8. Pseudoequilibrium modulus, G_N°, as a function of zwitterion content for AB (○) and AB′ (●) zwitterionomers.

zwitterionomers compared to the PBA zwitterionomers. It may also reflect a greater heterogeneity in the two phases in the former compared to the latter. It is only when $LiClO_4$ is added to the PEA zwitterionomers that the rheological behavior resembles that in the salt-free PBA zwitterionomers. There, a minimum in the G'' curves is observed, and it also becomes shallower with increasing zwitterion content. However, there is still no clear evidence of a constant slope in G' or G'' following the rubbery zone.

Equilibrium Modulus. The pseudoequilibrium modulus of the entanglement network, G_N°, can be calculated according to the equation[18,19]

$$G_N^\circ = (2/\pi)[2.3 \int_{-\infty}^{a} G''(\omega)\, d \log \omega] \quad (1)$$

where a terminates the integration before the transition zone is entered. These values are shown as a function of zwitterion content in Figure 8. When calculated from the relation $G_N^\circ = G'(\omega^*)$, where ω^* is the frequency corresponding to the loss tangent minimum, the values are within 10% of those calculated from eq 1. The value for the $LiClO_4$-containing sample is not so different from that for the salt-free sample; this was also observed for the PEA zwitterionomers.[4] Figure 8 shows that G_N° increases with mol % zwitterion content, F_B, according to the law $G_N^\circ \propto F_B^n$ where $n = 2.2$ (compared to 1.5 for the PEA zwitterionomers).

To rationalize the rise in modulus and the increasing width of the rubbery plateau with zwitterion content, it is possible to envisage two extreme situations. In the first, the ionic aggregates or hard phase in the zwitterionomers are considered as reinforcing filler. As long as the zwitterion content is not too high, this situation can be pictured as a viscoelastic matrix within which spherical viscoelastic inclusions are dispersed. When the matrix is rubbery, with a modulus $G_N^\circ(A_n)$, and the inclusions have a comparatively high modulus (in the present case, this can be considered to be on the order of 10^9 Pa for temperatures below T_g^H), the complex modulus, G^*, which can be calculated[20] for the material, reduces to its purely elastic component in the region between the two transitions:

$$G = G_N^\circ(A_n)[(1+1.5\Phi)/(1-\Phi)] \quad (2)$$

where, according to ref 21, $G_N^\circ(A_n) = 1.7 \times 10^5$. The volume fraction, Φ, can be taken to correspond to the volume fraction of the hard domains (Φ^H) calculated from DSC data for the copolymers which show two T_g's or, for AB-2.0 and AB-4.0 which show one T_g by DSC, to the volume fraction of the B counits (Φ_B) (Table I).[8] Table II shows that the G values calculated from eq 2 are much smaller than the G_N° values determined using eq 1, the difference increasing drastically with increasing zwitterion content. This demonstrates that it is simplistic to consider the hard domains acting simply as reinforcing filler particles, even at low zwitterion contents.

At the other extreme, the associated zwitterion units can be considered as thermoreversible cross-link points, thus forming a temporary network structure. With this point of view, the G_N° values determined from eq 1 can be used to calculate ν_e, the number of temporary network strands per unit volume, M_e, the average molecular weight of the temporary network strands, and $(\bar{r_0^2})^{0.5}$, their unperturbed root-mean-square end-to-end distance, from the following classical equations:[18,22]

$$\nu_e = 5G_m/4kT \quad (3)$$

$$M_e = 4\rho RT/5G_m \quad (4)$$

where k is Boltzmann's constant, R is the gas constant, ρ is the sample density,

$$G_m = G_{matrix} = G_N^\circ[(1+1.5\Phi)/(1-\Phi)]^{-1} \quad (5)$$

and

$$(\bar{r_0^2})^{0.5} = (K_\theta/\Phi_0)^{1/3} M_e^{1/2} \quad (6)$$

where K_θ are the unperturbed dimensions and Φ_0 is the Flory constant. These equations are valid subject to the following hypotheses: (a) the modulus, G_m, presumed to characterize the PBA matrix, is related to the equilibrium modulus, G_N°, calculated from the experimental data using eq 1 and taking into account Φ_B and Φ^H as explained above; (b) the network strands have an essentially Gaussian conformation;[23] and (c) the unperturbed chain dimensions are determined from intrinsic viscosity–molecular weight ($[\eta]$–$\bar{M}_w$) data for poly(*n*-butyl acrylate) solutions in acetone at 25 °C,[24] which gives $[\eta]$ (mL g^{-1}) $= 6.8 \times 10^{-3} \bar{M}_w^{0.75}$, and $K_\theta = 8.31 \times 10^{-2}$ mL g^{-1} is determined from the Stockmayer–Fixman–Burchardt equation.[25]

The results of the calculations (ν_{eq}, G_m, M_e, and $(\bar{r_0^2})^{0.5}$) are shown in Table II. The Bragg spacings, d_{SAXS}, determined from the small-angle X-ray scattering peak[8] are also included in Table II, for comparison with $(\bar{r_0^2})^{0.5}$. The latter two values can be reconciled by taking into account that the diffusing entities, if assumed to be spheres, have a radius[8] of *ca.* 20 Å; if d_{SAXS} represents the correlation distances between the centers of these entities, it is then approximately equal to $(\bar{r_0^2})^{0.5} + 2R$.

On the other hand, for the higher zwitterion contents, the values of ν_e are unrealistically high and those of M_e low; this indicates that the temporary cross-link model also becomes too simplistic as the hard-phase volume increases in importance. As is generally postulated for ionomers,[5-7] the modulus increase can better be attributed to a combination of filler and temporary network structures. The modulus may be enhanced as well by additional

entanglements that are trapped by the zwitterion aggregation process, as suggested for model polyurethane ionomers.[26]

It is of interest to compare the experimentally determined M_e values with the equivalent weight, M_e', of the zwitterionomers. When all of the zwitterions participate in simple ionic cross-links or multiplets (with no clustering), these two values should be approximately equal; by contrast, an increase in the ratio M_e'/M_e to above unity can be related to the development of significant clustering.[11] These ratios for the PBA zwitterionomers studied are tabulated in Table II and are observed to increase with zwitterion content. This increase is very similar to that which was observed for the previously mentioned styrene ionomers[11] with ionic groups located at the end of long pendant chains. In the latter case, the ratio increased from 0.85 for a 2.5 mol % ionomer to 2.6 for an 11 mol % ionomer. Comparison between the ratios for these long side-chain ionomers with those for styrene sodium methacrylate ionomers, for which the ratio increases much more rapidly with ion content (the ratio was determined to be 3.6 at 8 mol % ion content[11]), was taken as evidence that the former are much less clustered than the latter. It can be concluded that the PBA zwitterionomers are also less clustered than the styrene sodium methacrylate ionomers at comparable ion contents, but to a similar extent as in the long side-chain ionomers.

This is consistent with the results of DSC analysis of the PBA zwitterionomers, which indicate that the volume fraction of the cluster or hard phase is similar to that of the soft phase at about 25 mol % zwitterion content,[8] compared to 6 mol % ion content for styrene sodium methacrylate ionomers[14] (this comparison must be taken as approximate, since the methods used in estimating these values are not the same in both cases). The dominance of the soft phase compared to the hard phase may also explain, at least in part, the thermorheological simplicity observed for the zwitterionomers (up to AB-12.8 for which the volume fraction of the hard phase is 0.20) of this study in the frequency range investigated.

The fact that the zwitterions are located some distance from the polymer backbone, as well as their high dipole moment, should favor the formation of larger multiplets,[27] and hence a smaller cluster volume per zwitterion,[28] compared to ionomers whose ionic groups are close to the polymer backbone. Small-angle X-ray scattering data for the zwitterionomers[8] indeed suggest that the zwitterionic aggregates are relatively large, as indicated by the fact that the Bragg distances, d_{SAXS}, are significantly greater than those for styrene sodium methacrylate ionomers [e.g., 65 Å for AB-7.1 (Table II) compared to 23 Å for the 6 mol % ionomer[28]]. More specifically, an upper limit for the average number of zwitterions per multiplet can be obtained from a crude space-filling calculation, assuming that d_{SAXS} (Table II) represents the center-to-center distance between multiplets and that all zwitterions participate in multiplets.[27] For AB-12.8, this calculation gives 93 zwitterions per multiplet, comparable to what was calculated for the ionomers with long spacers.[27]

The possibility that the strong ionic interactions in zwitterionomers give rise to large multiplet-like structures is also supported by melt rheological[29] and synchrotron X-ray[30] studies of narrow distribution polyisoprenes functionalized at one end by a sulfozwitterion; these studies not only indicate the existence of extended aggregates but show that these aggregates have long-range order, ranging from tubular structures arranged on a two-dimensional hexagonal lattice for low molecular weights to structures

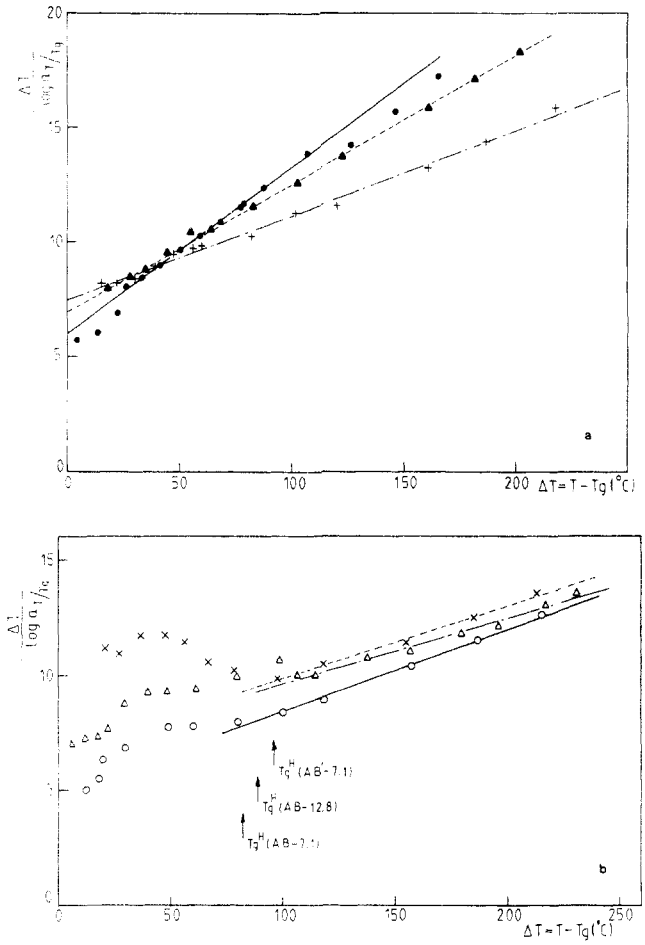

Figure 9. Temperature dependence of the shift factors (WLF test) used in constructing the master curves reduced to T_g^S for the following: (a) ●, A; ▲, AB-2.0; +, AB-4.0; (b) ○, AB-7.1; ×, AB-12.8; △, AB'-7.1.

arranged on a body-centered-cubic lattice for higher molecular weights. Such long-range order would not be expected in the statistical zwitterionomers of this study, where steric hindrances are much more restrictive (this is confirmed by SAXS measurements,[8] which show only the usual single broad peak typical of ionomers); nevertheless, there may be similar tendencies to form large zwitterionic aggregates in statistical and semitelechelic zwitterionomers.

Shift Factors. The horizontal shift factors, a_T, necessary for constructing the master curves are plotted in Figure 9 in a form which tests the validity of the WLF equation (with T_g or T_g^S as the reference temperature). Two distinct types of behavior are visible. At low zwitterion contents (Figure 9a), the WLF equation appears valid in the entire temperature range investigated (scatter in the points for pure PBA can be attributed to the experimental difficulties in obtaining good data for this sample). At higher zwitterion contents (Figure 9b), including the $LiClO_4$-containing sample, there is significant deviation from WLF behavior in the region which corresponds to the temperature range *below* the glass transition (DSC) of the hard phase (identified in Figure 9); the WLF equation appears to hold in the temperature range above this transition. It is noteworthy that the zwitterionomer composition for which the shift factor behavior becomes complex is also that for which two T_g's are first detected by DSC.

The slope of the best line through the points for each sample decreases with increasing zwitterion content up to AB-4.0, after which it remains relatively constant (in-

Table III. WLF Constants (c_1^g, c_2^g), Thermal Expansion Coefficient (α_f), and Fractional Free Volume (f_g) at T_g or T_g^S

sample	c_1^g	c_2^g (K)	$10^4\alpha_f$ (K^{-1})	f_g	R (x)[a]
A	13.8	83	3.8	0.031	0.999 (10)
AB-2.0	17.9	124	1.9	0.024	0.999 (13)
AB-4.0	27.0	201	0.8	0.016	0.996 (13)
AB-7.1	28.0	137	1.1	0.015	0.998 (6)[b]
AB-12.8	31.8	214	0.6	0.014	0.997 (5)[b]
AB'-7.1	35.3	239	0.5	0.012	0.991 (8)[b]

[a] R, correlation coefficient using (x) data points. [b] Calculations using only the points that form the linear portion of the curves shown in Figure 9.

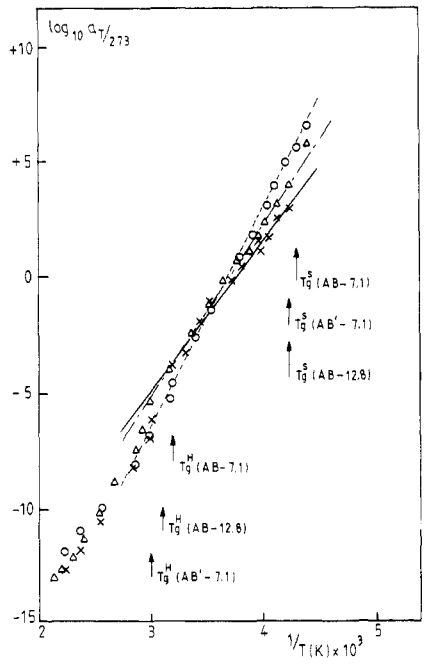

Figure 10. Temperature dependence of the shift factors according to an Arrhenius equation (with 0 °C as the reference temperature): ○, AB-7.1; ×, AB-12.8; △, AB'-7.1.

cluding for the salt-containing sample). This may be related to the small change in composition of the hard domains for the higher zwitterion contents, as indicated by the values for W_B^H in Table I. The WLF constants c_1^g and c_2^g, the thermal expansion coefficients α_f, and the fractional free volumes f_g (at T_g^S or the matrix T_g) for the different samples are listed in Table III.

The temperature region below T_g^H for the copolymers showing deviation from WLF behavior is analyzed in Figure 10 by an Arrhenius plot, using 0 °C as the reference temperature. It is observed that the behavior indeed appears Arrhenius in this region. The apparent activation energies corresponding to the slopes of the best straight lines through the points are 79, 61, and 54 kJ mol^{-1} for AB-7.1, AB'-7.1, and AB-12.8, respectively.

The shift factor behavior of the PBA zwitterionomers contrasts with that for the PEA zwitterionomers. In the latter case, when salt-free, the WLF equation is valid over the entire temperature range for all of the zwitterion contents studied (up to 15 mol %). The slopes are similar in all cases. Only when $LiClO_4$ is added do the samples show two temperature regions with distinct behaviors; however, each region could be fitted with a separate WLF equation.

Conclusions

The general features of the dynamic mechanical properties of the PBA zwitterionomers studied here qualitatively resemble those of biphasic ionomers,[5,6,31] including biphasic butyl acrylate-based cationomers.[13,32] Significant changes occur in the transition, rubbery, and terminal zones when zwitterionic units are incorporated. There is clear evidence for two dispersion regions for all zwitterion contents investigated, one corresponding to the T_g of a soft phase and the other to the T_g of a hard phase. The relative importance of the soft and hard phases decreases and increases, respectively, as zwitterion content increases. In particular, the loss tangent associated with T_g^S decreases significantly in intensity and area with increasing zwitterion content. The apparent Arrhenius activation energy of T_g^H is also lower than that of T_g^S (as determined by DMTA). A distinct rubbery plateau zone appears, and storage and loss moduli increase with zwitterion content. In parallel, the flow zone is increasingly retarded to lower frequencies or higher temperatures, with the result that the rubbery zone is increasingly extended. This indicates very strong electrostatic interactions among the zwitterionic units.

Significant differences with ionomers and with PEA zwitterionomers are also evident. The T_g^S, for example, increases only slightly with zwitterion content; this may reflect the small concentration of zwitterions in the soft phase, as previously determined from DSC,[8] compared to most ionomers. The T_g^H is reflected most clearly in the loss modulus curves; the loss tangent curves show no peak but only a high, very slowly increasing loss over a wide temperature range. In this temperature range, the moduli are observed to give a constant slope (whose value depends on zwitterion content) as a function of frequency. This feature has rarely been observed before. The flow zone was attained for all the samples studied.

The phase separation in PBA zwitterionomers appears to be better defined than in most ionomers. These are the first such materials for which two T_g's are clearly and easily evident by DSC.[8] They correspond to the two dispersion regions observed in the dynamic mechanical analysis of the present study. However, whereas the DSC T_g^H was detected only for zwitterion contents of 4.6 mol % and higher,[8] the dispersion region corresponding to the hard phase was observed dynamic mechanically at all zwitterion contents studied, including 2 mol %. Analysis of the rubbery moduli indicates that the extent of clustering is similar to that observed in ionomers with long spacers between the ionic group and the polymer backbone and significantly less than in ionomers with ionic groups very near the polymer backbone.[11] On the other hand, the data suggest that the multiplets in the zwitterionomers are large.

The addition of a stoichiometric amount of $LiClO_4$ to the PBA zwitterionomer has a relatively small effect on its dynamic mechanical properties. The second dispersion zone is displaced to somewhat higher temperatures or lower frequencies and causes the terminal zone to be unattainable before degradation sets in. However, the height of the rubbery plateau is unaffected by the salt. Although the effect of added $LiClO_4$ on the previously studied PEA zwitterionomers was similar in quality, the rubbery plateau zone of the latter was extended by the salt much more significantly. The addition of salt thus appears not to affect the extent of phase segregation; rather, it strengthens the aggregates or increases their lifetimes, thereby retarding flow.

Finally, no evidence of thermorheological complexity was found in any of the zwitterionomers studied, either with or without added salt. On the other hand, the shift factors fit a single WLF equation only for the 2 and 4 mol % zwitterionomers. For the higher zwitterion contents

studied and the zwitterionomer with added salt, only the higher temperature (or lower frequency) regions can be fitted by a WLF equation, whereas the lower temperature (or higher frequency) region is better fit by an Arrhenius equation.

Acknowledgment. The authors are grateful to Rhone-Poulenc for a grant to M.E. The contribution from Laval University was supported financially by NSERC (Canada) and FCAR (Quebec). Xia Tong (Laval University) is thanked for performing the DMTA measurements. Fruitful discussions with Drs. D. Charmot, J. C. Daniel, and R. Reeb (Rhone-Poulenc, Centre de Recherches d'Aubervilliers) are also acknowledged.

References and Notes

(1) Graiver, D.; Litt, M.; Baer, E. *J. Polym. Sci., Polym. Chem. Ed.* **1979**, *17*, 3607.
(2) Salamone, J. C.; Mahmud, N. A.; Mahmud, M. U.; Nagabhushanam, T.; Watterson, A. C. *Polymer* **1982**, *23*, 843.
(3) Speckhard, T. A.; Hwang, K. K. S.; Yang, C. Z.; Laupan, W. R.; Cooper, S. L. *J. Macromol. Sci., Phys.* **1984**, *B23* (2), 175.
(4) Bazuin, C. G.; Zheng, Y. L.; Muller, R.; Galin, J.-C. *Polymer* **1989**, *30*, 654.
(5) Eisenberg, A.; King, M. *Ion-Containing Polymers*; Academic Press: New York, 1977.
(6) Tant, M. R.; Wilkes, G. L. *J. Macromol. Sci., Rev. Macromol. Chem. Phys.* **1988**, *C28* (1), 1.
(7) Eisenberg, A.; Hird, B.; Moore, R. B. *Macromolecules* **1990**, *23*, 4098.
(8) Ehrmann, M.; Mathis, A.; Meurer, B.; Scheer, M.; Galin, J.-C. *Macromolecules* **1992**, *25*, 2253.
(9) Ehrmann, M.; Galin, J.-C.; Meurer, B. *Macromolecules* **1993**, *26*, 988.
(10) Ehrmann, M.; Galin, J.-C. *Polymer* **1992**, *33*, 859.
(11) Gauthier, M.; Eisenberg, A. *Macromolecules* **1990**, *23*, 2066.
(12) Murali, R.; Eisenberg, A. In *Structure and Properties of Ionomers*; Pineri, M., Eisenberg, A., Eds.; NATO Advanced Study Institute Series C198; Reidel Publishing Co.: Dordrecht, The Netherlands, 1987; p 307.
(13) Duchesne, D.; Eisenberg, A. *Can. J. Chem.* **1990**, *68*, 1228.
(14) Hird, B.; Eisenberg, A. *J. Polym. Sci., Polym. Phys. Ed.* **1990**, *28*, 1665.
(15) This hypothesis is supported by results concerning selective plasticization of the PBA zwitterionomers: Galin, M.; Mathis, A.; Galin, J.-C. *Macromolecules*, following paper in this issue.
(16) Bazuin, C. G.; Eisenberg, A.; Kamal, M. *J. Polym. Sci., Polym. Phys. Ed.* **1986**, *24*, 1155.
(17) Stadler, R.; de Lucca Freitas, L. L. *Colloid Polym. Sci.* **1986**, *264*, 773.
(18) Ferry, J. D. *Viscoelastic Properties of Polymers*, 3rd ed.; John Wiley & Sons: New York, 1980.
(19) de Lucca Freitas, L. L.; Stadler, R. *Macromolecules* **1987**, *20*, 2478.
(20) Palierne, J. F. *Rheol. Acta* **1990**, *29*, 204.
(21) Cavaille, J. Y.; Jourdan, C.; Kong, X. Z.; Perez, J.; Pichot, C.; Guillot, J. *Polymer* **1986**, *27*, 693.
(22) Flory, P. J. *Principles of Polymer Chemistry*; Cornell University Press: Ithaca, NY, 1953.
(23) Squires, E.; Howe, S.; Painter, P. *Macromolecules* **1987**, *20*, 1740.
(24) Saini, G.; Trossarelli, L. *Atti Accad. Sci. Torino, Cl. Sci. Fis. Mat. Nat.* **1955**, *90*, 410.
(25) Stockmayer, W. H.; Fixman, M. *J. Polym. Sci.* **1963**, *C-1*, 137.
(26) Visser, S. A.; Cooper, S. L. *Macromolecules* **1991**, *24*, 2576.
(27) Moore, R. B.; Bittencourt, D.; Gauthier, M.; Williams, C. E.; Eisenberg, A. *Macromolecules* **1991**, *24*, 1376.
(28) Hird, B.; Eisenberg, A. *Macromolecules* **1992**, *25*, 6466.
(29) Fetters, L. J.; Graessley, W. W.; Hadjichristidis, N.; Kiss, A. D.; Pearson, D. S.; Younghouse, L. B. *Macromolecules* **1988**, *21*, 1644.
(30) Shen, Y.; Safinya, C. R.; Fetters, L.; Adam, M.; Witten, T.; Hadjichristidis, N. *Phys. Rev. A* **1991**, *43*, 1886.
(31) Weiss, R. A.; Fitzgerald, J. J.; Kim, D. *Macromolecules* **1991**, *24*, 1071.
(32) Otocka, E. P.; Eirich, F. R. *J. Polym. Sci., Polym. Phys. Ed.* **1968**, *6*, 933.